



Deposited via The University of Leeds.

White Rose Research Online URL for this paper:

<https://eprints.whiterose.ac.uk/id/eprint/82695/>

Version: Accepted Version

Article:

Wang, Y, Wang, F, Guo, Y et al. (2014) Controlled synthesis of monodisperse gold nanorods with different aspect ratios in the presence of aromatic additives. *Journal of Nanoparticle Research*, 16 (12). 2806. ISSN: 1572-896X

<https://doi.org/10.1007/s11051-014-2806-3>

Reuse

Items deposited in White Rose Research Online are protected by copyright, with all rights reserved unless indicated otherwise. They may be downloaded and/or printed for private study, or other acts as permitted by national copyright laws. The publisher or other rights holders may allow further reproduction and re-use of the full text version. This is indicated by the licence information on the White Rose Research Online record for the item.

Takedown

If you consider content in White Rose Research Online to be in breach of UK law, please notify us by emailing eprints@whiterose.ac.uk including the URL of the record and the reason for the withdrawal request.

1 **Controlled synthesis of monodisperse gold nanorods with**
2 **different aspect ratios in the presence of aromatic additives**

3 Yun Wang • Feihu Wang • Yuan Guo • Rongjun Chen • Yuanyuan Shen • Aijie Guo • Jieying Liu • Xiao Zhang
4 • Dejian Zhou • Shengrong Guo

5 Y. Wang • F. Wang • Y. Shen • A. Guo • J. Liu • X. Zhang • S. Guo (✉)

6 School of Pharmacy, Shanghai Jiao Tong University, 800 Dongchuan Road, Shanghai 200240, P. R. China

7 E-mail: srguo@sjtu.edu.cn or s.guo@leeds.ac.uk (S.G.)

8 Tel / Fax: + 86 21 34204793

9 Y. Guo • S. Guo • D. Zhou (✉)

10 School of Chemistry and Astbury Centre for Structural Molecular Biology, University of Leeds, Leeds LS2 9JT,

11 United Kingdom

12 E-mail: d.zhou@leeds.ac.uk (D.Z.)

13 R. Chen

14 Department of Chemical Engineering, Imperial College London, South Kensington Campus, London 11 SW7 2AZ,

15 United Kingdom

16 E-mail: rongjun.chen@imperial.ac.uk

17
18 **Abstract** This paper reports the synthesis of monodisperse gold nanorods (GNRs) *via* a simple seeded growth
19 approach in the presence of different aromatic additives, such as 7-bromo-3-hydroxy-2-naphthoic acid (7-BrHNA),
20 3-hydroxy-2-naphthoic acid (HNA), 5-bromosalicylic acid (5-BrSA), salicylic acid (SA) or phenol (PhOH). Effects of
21 the aromatic additives and hydrochloric acid (HCl) on the structure and optical properties of the synthesized GNRs
22 were investigated. The longitudinal surface plasmon resonance (LSPR) peak wavelength of the resulting GNRs was
23 found to be dependent on the aromatic additive in the following sequence: 5-BrSA (778 nm) > 7-BrHNA (706 nm) >
24 SA (688 nm) > HNA (676 nm) > PhOH (638 nm) without addition of HCl, but this was changed to 7-BrHNA (920 nm) >
25 SA (890 nm) > HNA (872 nm) > PhOH (858 nm) > 5-BrSA (816 nm) or 7-BrHNA (1005 nm) > PhOH (995 nm) > SA

26 (990 nm) > HNA (980 nm) > 5-BrSA (815 nm) with the addition of HCl or HNO₃ respectively. The LSPR peak
27 wavelength was increased with the increasing concentration of 7-BrHNA without HCl addition, however, there was a
28 maximum LSPR peak wavelength when HCl was added. Interestingly, the LSPR peak wavelength was also increased
29 with amount of HCl added. The results presented here thus established a simple approach to synthesize monodisperse
30 GNRs of different LSPR wavelength.

31

32 **Keywords:** Gold nanorod • Seeded growth • Aromatic additive • LSPR peak wavelength • HCl

33

34 **Introduction**

35

36 Gold nanorods (GNRs) exhibit two distinct optical adsorption bands stemming from the longitudinal and transverse
37 surface plasmon resonances (LSPR and TSPR) (Sharma et al. 2009). The maximum LSPR absorption wavelength is
38 linearly related to the aspect ratio (AR: ratio of length to diameter) of the GNRs (Charan et al. 2012; Lohse and
39 Murphy 2013; Menon et al. 2012; Ye et al. 2012). The GNRs, with unique AR-dependent optical properties, have
40 attracted a great deal of interests in many research areas, including bioprobe (Tian et al. 2012), biomedical imaging
41 (Charan et al. 2012; Wang et al. 2013), spectroscopic detection (Huang et al. 2012), drug delivery (Zhong et al. 2013),
42 gene therapy (Wang et al. 2013; Xu et al. 2013) and photothermal therapy (Liu et al. 2014; Song et al. 2013; Wang et al.
43 2011).

44 GNRs are generally synthesized *via* a seed-mediated growth method (Grzelczak et al. 2008) pioneered by Murphy
45 et al. (2001), improved by El-Sayed et al. (2003), and then developed by Ye et al. (2012). Surfactants are commonly
46 used in such a method, and the most widely used surfactant being cetyltrimethylammonium bromide (C16TABr)
47 (Gomez-Grana et al. 2011). It was proposed that GNRs are stabilized by a partially-interdigitated bilayer of C16TABr
48 (Gomez-Grana et al. 2011; Johnson et al. 2002; Murphy et al. 2005). The anisotropic growth of the GNRs is due to the
49 preferential binding of the cetyltrimethylammonium⁺ (C16TA⁺) head group to the {110} face of the seed gold
50 nanoparticle as it has higher surface energies than other faces (Gai and Harmer 2002; Huang et al. 2009). C16TABr
51 binding stabilizes this face and consequently crystal growth on this face is retarded. As a result, gold atoms are
52 preferentially deposited to the two end facets, leading to rod growth. This mechanism is also supported by density
53 functional theory simulation recently reported by Almora-Barrios et al. (2014).

Comment [y1]: Cite Feihu's JCR paper, which has already has the page numbers

Comment [y2]: Inaccurate, use "adsorption"

54 It has been found that the micellization behavior of C16TABr surfactant can be modified *via* adding certain
55 aromatic compounds (Yoo et al. 2010). Ye et al. (2012) proved that some aromatic additives can mediate the binding
56 between the C16TABr bilayers and certain facets of growing GNRs. The aromatic ring and carboxyl groups within the
57 additives are the possible binding sites to the surface gold (Michota and Bukowska 2003; Wang et al. 2010). The
58 interaction between halide ions and gold surfaces has also been investigated (Almora-Barrios et al. 2014; Si et al.
59 2012). Interestingly, bromide anion (Br^-) is hugely influential in the GNR growth. For example, Jin et al. (2010)
60 found that Br^- ion was a crucial shape-directing agent for GNR formation in the seed-mediated process, irrespective of
61 its origin (C16TABr or NaBr). The size and shape of GNRs could also be modulated by the pH (Edgar et al. 2012;
62 Wang et al. 2005; Ye et al. 2013; Zhu et al. 2010). An increase of OH^- ions of the growth solution could decrease the
63 amount of C16TA^+ surfactants adsorbed on the {110} face of the GNR (Wang et al. 2005). Despite of significant
64 research over the past 10 years, there have been contradictory reports about how pH may affect the GNR growth (Ye et
65 al. 2013; Ye et al. 2012; Zhu et al. 2010). Moreover, effects of different aromatic additives on the GNR shape and AR
66 are still not fully understood.

67 Herein, we have systematically studied how GNR growth can be affected by five different aromatic additives with
68 and without added hydrochloric acid (HCl) by the seeded growth method. We show that the pH and aromatic additives
69 are both important in determining the GNR AR and shape. It is possible to synthesis monodisperse GNRs with LSPR
70 spanning from ~660 nm to 960 nm.

71

72 **Experimental section**

73

74 **Materials**

75 The following chemicals were purchased commercially and used as received unless otherwise stated. Cetyltrimethyl-
76 ammonium bromide (C16TABr, $\geq 99\%$), 7-bromo-3-hydroxy-2-naphthoic acid (7-BrHNA, $\geq 98\%$), silver nitrate
77 (AgNO_3 , 99.9999%) and ascorbic acid (AA, reagent grade) were purchased from Sigma-Aldrich. 5-bromosalicylic
78 acid (5-BrSA, $>98.0\%$) was purchased from TCI Shanghai. 3-hydroxy-2-naphthoic acid (HNA, 98%) was purchased
79 from J&K Scientific Ltd. Salicylic acid (SA, 99.5%) and sodium borohydride (NaBH_4 , 98%) were purchased from
80 Aladdin. Phenol (PhOH, AR), chloroauric acid tetrahydrate ($\text{HAuCl}_4 \cdot 4\text{H}_2\text{O}$, AR), hydrochloric acid (HCl, 36.0 ~

81 38.0 wt % in water) and nitric acid (HNO_3 , 65 ~ 68 wt % in water) were purchased from Sinopharm Chemical Reagent
82 Co., Ltd. All solutions were prepared with deionized (DI) water.

83

84 Synthesis of GNRs by an improved seeded growth method using aromatic additives

85 The seed solution for GNR growth was prepared as reported previously (Nikoobakht and El-Sayed 2003). Briefly, a 5
86 mL solution of 0.5 mM HAuCl_4 was mixed with 5 mL of 0.2 M C16TABr solution. A 0.6 mL of freshly prepared 0.01
87 M ice-cold NaBH_4 aqueous solution was then injected into the Au^{3+} -C16TABr solution under vigorous stirring (1200
88 rpm). After 2 min, the stirring was stopped and the solution color changed from yellow to brownish-yellow. The seed
89 solution was aged at 30°C for 1.5 hours before use.

90 For the preparation of the growth solution, 0.54 g of C16TABr together with a certain amount of each additive
91 were dissolved in 15 mL of warm water (~ 60°C) in a 50 mL erlenmeyer flask (Ye et al. 2012). The solution was then
92 cooled to 30°C when a 4 mM AgNO_3 solution was added. The mixture was kept undisturbed at 30°C for 15 min, after
93 which 15 mL of 1 mM HAuCl_4 solution and a small amount of HCl (12.1 M) was added. After 15 min of slow stirring
94 (400 rpm), 0.064 M AA was added, and then vigorously stirred for 30 s until the solution color became uniform and
95 stable.

96 At last, the seed solution was injected into the growth solution. The resultant mixture was stirred for 30 s and then
97 left undisturbed at 30°C for 12 hours for the GNR growth. The resulting GNRs were separated from the reaction
98 solution *via* centrifugation at 11500 rpm for 25 min, washed with deionized water twice to remove any residual
99 reactants. The precipitates were re-dispersed in 2 mL of deionized water.

100

101 Characterization

102 Ultraviolet-visible-near infrared (UV-vis-NIR) spectra were recorded on a Hitachi U-2910 UV-vis-NIR
103 spectrophotometer. The morphology and size of the GNRs were measured using transmission electron microscopy
104 (TEM) (JEM-2100F, JEOL, Japan).

105

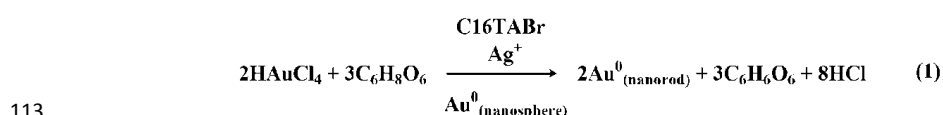
106

107 **Results and discussion**

108

109 Effects of aromatic additives

110 GNRs are mostly prepared *via* a seeded growth approach using small gold nanoparticle seeds in the presence of
111 C16TABr in aqueous media. The overall chemical reaction (Edgar et al. 2012) for the GNR synthesis can be described
112 in Equation (1) below:



114 Where $\text{C}_6\text{H}_8\text{O}_6$ is AA, a reducing agent that is oxidized to dehydroascorbic acid ($\text{C}_6\text{H}_6\text{O}_6$) after the reaction and
115 C16TABr is used to direct GNR formation.

116 In a typical 'seeded' growth process, GNRs are prepared by adding gold nanoparticle seeds to an aqueous 'growth
117 solution' which consists of a mixture of C16TABr, HAuCl_4 , AA, and silver nitrate (Edgar et al. 2012; Nikoobakht and
118 El-Sayed 2003). A number of factors that affect the GNR synthesis have been investigated. These include temperature,
119 pH, gold nanoparticle seed, reactant concentration, single-component surfactant other than C16TABr, binary
120 surfactant mixtures *etc.* (Edgar et al. 2012; Lai et al. 2014; Murphy et al. 2010; Wadams et al. 2013; Wang et al. 2005;
121 Ye et al. 2013; Zhu et al. 2010). More recently, Ye et al. (2012) reported that monodispersity and spectral tunability of
122 GNR could be achieved by using SA or 5-BrSA as additive. It might be because such aromatic additives can be
123 embedded within the C16TABr capping layers of GNRs, leaving the polar groups pointing away from the hydrocarbon
124 chain of C16TABr (Hassan and Yakhmi 2000; Lin et al. 1994), although the detailed mechanism is still unclear. Herein,
125 we have investigated effects of 5 different aromatic compounds with different functional groups and aromatic rings on
126 the synthesis of GNRs in an attempt to find out most effective additives. The chemical structures and structural
127 characteristics of these aromatic additives are shown in Fig. 1 and Table 1. These compounds contain two different
128 aromatic rings (benzene and naphthalene ring) and 3 different functional groups (-Br, -COOH and -OH).

129 Without addition of HCl, the prepared GNR aqueous solutions are different in color, from red to blue, dependent
130 on the aromatic additives. Fig. 2 shows that the synthesized GNRs are relatively monodisperse and their UV-vis-NIR
131 spectra all show two distinct absorption bands, a weaker band peaking at about 525 nm and a stronger band peaking at

132 a longer wavelength. These two bands are attributed to TSPR and LSPR, respectively. A close look of the GNR TEM
133 images reveals that the GNRs prepared in the presence of PhOH, SA, HNA, or 7-BrHNA are stubby sausage- or dog
134 bone-like shapes. Only those prepared in the presence of 5-BrSA are long cylindrical shape rod-like.

135 The concentrations, pH, dimensions, AR and LSPR peak wavelengths of the GNR solutions prepared in the
136 presence of aromatic additives are summarized in Table 2. The AR of the GNRs was measured from the TEM images
137 in Fig. 2a-e. The LSPR peak wavelength (λ_{LSPR}) of the GNRs is found to be positively and linearly correlated to the AR
138 *via* equation (2) below:

$$139 \quad \lambda_{LSPR} = 112.5 \times AR + 411.4 \quad (2)$$

140 The above equation clearly indicates that the LSPR peak wavelength is strongly dependent on the AR of GNRs (Lohse
141 and Murphy 2013): the bigger the AR, the longer the LSPR peak wavelength of GNRs. The TEM images of GNRs
142 (Fig. 2a-e) are well correlated with their UV-vis-NIR spectra (Fig. 2f).

143 As shown in Table 2, the GNR LSPR peak wavelength is found to be dependent on the aromatic additives in the
144 following order: PhOH (638 nm) < SA (688 nm) < 5-BrSA (778 nm) and HNA (676 nm) < 7-BrHNA (706 nm). PhOH,
145 SA and 5-BrSA all have the same aromatic ring (benzene), while HNA and 7-BHNA are both naphthalene derivatives.
146 The differences in the LSPR peak wavelengths obtained here should be mainly due to the functional groups on
147 aromatic ring, and it appears that introduction of the -Br and -COOH groups to the aromatic rings is beneficial for
148 making GNRs with high ARs (long LSPR peak wavelengths).

149 The LSPR peak wavelengths of GNRs synthesized using 5-BrSA or 7-BrHNA are longer than those without -Br.
150 Thus, aromatic additives with a Br group may facilitate the preparation of high AR GNRs, possibly due to a relatively
151 strong affinity of the Br atom with Au. Comparing the additives with the same functional group(s), GNRs synthesized
152 with 5-BrSA has a longer LSPR peak wavelength than that with 7-BrHNA, and this is also true for SA and HNA. This
153 indicates that the aromatic rings (benzene and naphthalene) in the additives also play a certain role in determining the
154 AR of the GNRs, possibly due to the different affinity of the aromatic rings to Au. Unlike the other 4 aromatic
155 additives, PhOH does not contain a -COOH group and hence is a much weaker acid (pKa ~9) compared to others all
156 containing a -COOH group (pKa ~4-5). As a result, the pH value of the resulting GNR solution with PhOH is higher
157 (pH 3.00) than others (*ca* 2.5, see Table 2). The solution pH has been found to influence the AR (hence LSPR peak
158 wavelength) of the synthesized GNRs (Wang et al. 2005; Ye et al. 2012; Zhu et al. 2010).

159

160 Effect of HCl

161 The effects of the aromatic additives on the GNR synthesis were changed dramatically when 300 μL (~36 mmol) of
162 concentrated HCl solution was added in the growth solution (Fig. 2, 3). The synthesized GNR solutions were light
163 brown to light red and the GNRs were mostly cylindrical shape. Concentrations and LSPR peak wavelengths of the
164 GNRs in the final solutions are listed in Table 3. Compared to Table 2, the concentrations of resulting GNRs are
165 decreased from 0.87-0.89 to 0.61 nM for SA, HNA and 7-BrHNA after addition of HCl. However, the GNR
166 concentration with 5-BrSA is increased from 0.22 to 0.67 nM, while that for PhOH additive shows little difference.
167 The LSPR peak wavelength orders for the GNR solutions are as follows: 7-BrHNA (920 nm) > SA (890 nm) > HNA
168 (872 nm) > PhOH (858 nm) > 5-BrSA (816 nm). This order is completely different from that obtained without addition
169 of HCl as mentioned above. Moreover, the LSPR bands are stronger and also appear at longer wavelengths. This
170 indicates that the effect of HCl on the synthesized GNRs is significant even in the presence of aromatic additives. This
171 is unsurprisingly given the fact the formation of GNR (Equation 1) does release HCl into the reaction media. In
172 addition, many other factors could also influence the GNR growth, including formation of AgBr (Huang et al. 2009;
173 Murphy et al. 2010), aromatic electron system on the GNR surfaces (Michota and Bukowska 2003; Wang et al. 2010),
174 and the reducing power of AA (Wang et al. 2005).

175 **The reduction of gold ions into gold atoms can be determined by monitoring the optical absorbance of the GNRs**
176 **growth solutions at 440 nm (Rao and Doremus 1996, Sau and Murphy 2004). The bigger the absorbance, the more the**
177 **gold atoms formed. The change of the absorbance of the GNRs growth solutions with time can reflect the reduction**
178 **kinetics of gold precursor in the GNRs growth solutions. After addition of 30 mmol HCl into the growth solutions with**
179 **different aromatic additives, the pH values of the resulting GNR growth solutions change from 2.5 ~ 3.0 to 1.2, the**
180 **times to reach the absorbance plateau value (about 1.1) are prolonged from about 10 min to 2 ~ 3 h (Fig. 4). This**
181 **indicates that the reduction of gold precursors is significantly slowed down. Wang ever reported that the decreasing pH**
182 **value of the GNR growth solution would lower the reducing power of AA and the reducing rate of gold ions (Wang et**
183 **al. 2005).**

184 The effects of the aromatic additives on the GNR synthesis were also changed dramatically when 36 mmol
185 concentrated HNO_3 solution was added in the growth solution (Fig. 5). The LSPR peak wavelengths for the prepared
186 GNRs solutions are in the following order: 7-BrHNA (1005 nm) > PhOH (995 nm) > SA (990 nm) > HNA (980 nm) >
187 5-BrSA (815 nm). The LSPR peak wavelengths obviously increase after the addition of HNO_3 , similar to that of HCl.

188 HNO_3 is a strong acid as HCl, but it does not contain halides. The pH values of the resulting GNR solutions with
189 addition of 36 mmol concentrated HNO_3 are 1.2. This indicates that pH plays a certain role in the process of GNR
190 growth. Given the fact that the LSPR peak appears at the highest wavelength (biggest AR) with 7-BrHNA after
191 addition of HCl or HNO_3 . In this case, the effect of 7-BrHNA concentration was further investigated.

192

193 Effects of 7-BrHNA concentration

194 As shown in Fig. 6, the LSPR band of GNR solution increases from 720 to 748 nm as the concentration of 7-BrHNA is
195 increased from 1.2 to 9.6 mM. Obviously, the concentration of the additive does have an impact on the GNR growth
196 and the LSPR wavelength. Without addition of HCl, there seems to have a trend that the more additive present in the
197 growth solution, the longer the LSPR peak wavelength for the obtained GNR. However, when HCl is added, there is a
198 maximum LSPR peak wavelength of 912 nm for GNR prepared at a certain concentration of 7-BrHNA (3.6 mM). At
199 the same concentration of 7-BrHNA, the LSPR is bigger after addition of HCl.

200

201 Effect of HCl amount

202 It remains a subject of considerable ongoing research interest how pH can be used to tune the LSPR wavelength of
203 GNRs despite several reported researches (Busbee et al. 2003; Cheng et al. 2011; Ye et al. 2013; Ye et al. 2012; Zhu et
204 al. 2010). Fig. 7 shows that the LSPR wavelength is increased from 894 to 932 nm with the amount of HCl added is
205 increased from 200 to 350 μL . This indicates that the ARs of GNRs synthesized in the presence of 3.6 mM 7-BrHNA
206 can be adjusted by changing amount of HCl added. The addition of HCl in the growth solution is beneficial for
207 preparing GNRs with bigger ARs and LSPR.

208

209 Controlled synthesis of GNRs

210 7-BrHNA is the most effective among the five aromatic additives studied here in terms of synthesizing GNRs with
211 high ARs and long LSPR absorption bands. Fig. 8 shows the absorption spectra of a range of GNRs synthesized with
212 7-BrHNA as additive, the LSPR bands of GNRs can be systematically adjusted from 660 to 960 nm by changing the
213 amount of reactants (see Fig. 8 and Table 4).

214

215 **Conclusion**

216 In summary, monodisperse GNRs are successfully synthesized *via* a seeded growth approach in the presence of
217 aromatic additive (PhOH, SA, 5-BrSA, HNA, or 7-BrHNA). The LSPR wavelength of the synthesized GNRs can be
218 systematically adjusted in the near infrared region, providing a facile, controllable way for preparation of GNRs with
219 desired optical properties that may have broad biomedical applications. 7-BrHNA, a -Br and -COOH containing small
220 aromatic additive, is the most effective among the five aromatic additives studied here in terms of synthesizing GNRs
221 with high ARs and long LSPR absorption bands.

222

223 **Acknowledgments** This work is supported by National Natural Science Foundation of China (NSFC, Grant
224 No.81171439), the National Key Technology R&D Program of the Ministry of Science and Technology
225 (2012BAI18B01) and the European Research Council via a Marie Curie International Incoming Fellowship to S.G.
226 (grant No. PIIF-GA-2012-331281). Y. Guo. thanks the Wellcome Trust (U.K.) for providing a Career Re-entry Fellowship
227 (Grant No: 097354/Z/11/Z).

228

229 **References**

230

231 Almora-Barrios N, Novell-Leruth G, Whiting P, Liz-Marzán LM, López N (2014) Theoretical description of the role
232 of halides, silver, and surfactants on the structure of gold nanorods. *Nano Lett* 14:871-875

233 Busbee BD, Obare SO, Murphy CJ (2003) An Improved Synthesis of High-Aspect-Ratio Gold Nanorods. *Adv Mater*
234 15:414-416

235 Charan S et al. (2012) Development of chitosan oligosaccharide-modified gold nanorods for in vivo targeted delivery
236 and noninvasive imaging by NIR irradiation. *Bioconjug Chem* 23:2173-2182

237 Cheng J, Ge L, Xiong B, He Y (2011) Investigation of pH Effect on Gold Nanorod Synthesis. *J Chin Chem Soc*
238 58:822-827

239 Edgar JA, McDonagh AM, Cortie MB (2012) Formation of gold nanorods by a stochastic “popcorn” mechanism. *ACS*
240 *Nano* 6:1116-1125

241 Gai PL, Harmer MA (2002) Surface atomic defect structures and growth of gold nanorods. *Nano Lett* 2:771-774

242 Garg N, Scholl C, Mohanty A, Jin R (2010) The role of bromide ions in seeding growth of Au nanorods. *Langmuir*
243 26:10271-10276

244 Gomez-Grana S, Hubert F, Testard F, Guerrero-Martínez A, Grillo I, Liz-Marzán LM, Spalla O (2011) Surfactant (bi)
245 layers on gold nanorods. *Langmuir* 28:1453-1459

246 Grzelczak M, Pérez-Juste J, Mulvaney P, Liz-Marzán LM (2008) Shape control in gold nanoparticle synthesis. *Chem*
247 *Soc Rev* 37:1783-1791

248 Hassan P, Yakhmi J (2000) Growth of cationic micelles in the presence of organic additives. *Langmuir* 16:7187-7191

249 Huang H, Li C, Qu C, Huang S, Liu F, Zeng Y (2012) Sensitive detection of DNA based on the optical properties of
250 core-shell gold nanorods. *J Nanopart Res* 14:1-7

251 Huang X, Neretina S, El-Sayed MA (2009) Gold nanorods: from synthesis and properties to biological and biomedical
252 applications. *Adv Mater* 21:4880-4910

253 Jana NR, Gearheart L, Murphy CJ (2001) Wet chemical synthesis of high aspect ratio cylindrical gold nanorods. *J*
254 *Phys Chem B* 105:4065-4067

255 Johnson CJ, Dujardin E, Davis SA, Murphy CJ, Mann S (2002) Growth and form of gold nanorods prepared by
256 seed-mediated, surfactant-directed synthesis. *J Mater Chem* 12:1765-1770

257 Lai J et al. (2014) One-pot synthesis of gold nanorods using binary surfactant systems with improved monodispersity,
258 dimensional tunability and plasmon resonance scattering properties. *Nanotechnology* 25:125601

259 Lin Z, Cai J, Scriven L, Davis H (1994) Spherical-to-wormlike micelle transition in CTAB solutions. *J Phys Chem*
260 98:5984-5993

261 Liu X, Huang N, Li H, Wang H, Jin Q, Ji J (2014) Multidentate Polyethylene Glycol Modified Gold Nanorods for in
262 Vivo Near-Infrared Photothermal Cancer Therapy. *ACS Appl Mater Interfaces* 6:5657-5668

263 Lohse SE, Murphy CJ (2013) The quest for shape control: a history of gold nanorod synthesis. *Chem Mater*
264 25:1250-1261

265 Menon D, Basanth A, Retnakumari A, Manzoor K, Nair SV (2012) Green synthesis of biocompatible gold
266 nanocrystals with tunable surface plasmon resonance using garlic phytochemicals. *J Biomed Nanotechnol*
267 8:901-911

268 Michota A, Bukowska J (2003) Surface-enhanced Raman scattering (SERS) of 4-mercaptobenzoic acid on silver and
269 gold substrates. *J Raman Spectrosc* 34:21-25

270 Murphy CJ et al. (2005) Anisotropic metal nanoparticles: synthesis, assembly, and optical applications. *J Phys Chem*
271 B 109:13857-13870

272 Murphy CJ et al. (2010) The many faces of gold nanorods. *J Phys Chem Lett* 1:2867-2875

273 Nikoobakht B, El-Sayed MA (2003) Preparation and growth mechanism of gold nanorods (NRs) using seed-mediated
274 growth method. *Chem Mater* 15:1957-1962

275 Orendorff CJ, Murphy CJ (2006) Quantitation of metal content in the silver-assisted growth of gold nanorods. *J Phys*
276 *Chem B* 110:3990-3994

277 Rao P and Doremus R (1996) Kinetics of growth of nanosized gold clusters in glass. *J Non Cryst Solids* 203:202-205.
278 doi: 10.1016/0022-3093(96)00483-8

279 Sau TK and Murphy CJ (2004) Seeded high yield synthesis of short Au nanorods in aqueous solution. *Langmuir*
280 20:6414-6420. doi: 10.1021/la049463z

281 Sharma V, Park K, Srinivasarao M (2009) Colloidal dispersion of gold nanorods: Historical background, optical
282 properties, seed-mediated synthesis, shape separation and self-assembly. *Mater Sci Eng R Rep* 65:1-38

283 Si S, Leduc C, Delville MH, Lounis B (2012) Short gold nanorod growth revisited: the critical role of the bromide
284 counterion. *ChemPhysChem* 13:193-202

285 Song J, Pu L, Zhou J, Duan B, Duan H (2013) Biodegradable theranostic plasmonic vesicles of amphiphilic gold
286 nanorods. *ACS Nano* 7:9947-9960

287 Tian Y, Chen L, Zhang J, Ma Z, Song C (2012) Bifunctional Au-nanorod@ Fe₃O₄ nanocomposites: synthesis,
288 characterization, and their use as bioprobes. *J Nanopart Res* 14:1-11

289 Wadams RC, Fabris L, Vaia RA, Park K (2013) Time-Dependent Susceptibility of the Growth of Gold Nanorods to the
290 Addition of a Cosurfactant. *Chem Mater* 25:4772-4780

291 Wang C-H, Chang C-W, Peng C-A (2011) Gold nanorod stabilized by thiolated chitosan as photothermal absorber for
292 cancer cell treatment. *J Nanopart Res* 13:2749-2758

293 Wang C, Wang T, Ma Z, Su Z (2005) pH-tuned synthesis of gold nanostructures from gold nanorods with different
294 aspect ratios. *Nanotechnology* 16:2555

295 Wang X, Shao M, Zhang S, Liu X (2013) Biomedical applications of gold nanorod-based multifunctional
296 nano-carriers. *J Nanopart Res* 15:1-16

297 Wang Z, Zong S, Yang J, Song C, Li J, Cui Y (2010) One-step functionalized gold nanorods as intracellular probe with
298 improved SERS performance and reduced cytotoxicity. *Biosens Bioelectron* 26:241-247

299 Xu C et al. (2013) Encapsulating gold nanoparticles or nanorods in graphene oxide shells as a novel gene vector. *ACS*
300 *Appl Mater Interfaces* 5:2715-2724

301 Ye X, Gao Y, Chen J, Reifsnnyder DC, Zheng C, Murray CB (2013) Seeded Growth of Monodisperse Gold Nanorods
302 Using Bromide-Free Surfactant Mixtures. *Nano Lett* 13:2163-2171

303 Ye X et al. (2012) Improved size-tunable synthesis of monodisperse gold nanorods through the use of aromatic
304 additives. *ACS Nano* 6:2804-2817

305 Yoo H, Sharma J, Yeh H-C, Martinez JS (2010) Solution-phase synthesis of Au fibers using rod-shaped micelles as
306 shape directing agents. *Chem Commun* 46:6813-6815

307 Zhong Y, Wang C, Cheng L, Meng F, Zhong Z, Liu Z (2013) Gold nanorod-cored biodegradable micelles as a robust
308 and remotely controllable doxorubicin release system for potent inhibition of drug-sensitive and-resistant
309 cancer cells. *Biomacromolecules* 14:2411-2419

310 Zhu J et al. (2010) Additive controlled synthesis of gold nanorods (GNRs) for two-photon luminescence imaging of
311 cancer cells. *Nanotechnology* 21:285106

312

313 **Table 1** Chemical structural characteristics of the five aromatic additives

Aromatic additive	aromatic ring	groups
PhOH	benzene	-OH
SA	benzene	-OH, -COOH
5-BrSA	benzene	-OH, -COOH, -Br
HNA	naphthalene	-OH, -COOH
7-BrHNA	naphthalene	-OH, -COOH, -Br

314

315

316 **Table 2** Comparison of the concentration, pH, dimensions, AR and LSPR peak wavelength of the GNR solutions
 317 prepared in the presence of different aromatic additive ^a

Additive ^b (g)	C ^c (nM)	pH	Dimensions ^d (nm)	AR	LSPR peak wavelength (nm)
PhOH	0.57	3.00	(37.3±2.2)×(17.4±1.4)	~2.1	638
SA	0.89	2.53	(46.3±4.6)×(19.3±2.6)	~2.4	688
5-BrSA	0.22	2.51	(45.1±3.4)×(13.6±1.1)	~3.3	778
HNA	0.87	2.50	(43.4±5.3)×(18.2±3.0)	~2.4	676
7-BrHNA	0.88	2.51	(47.0±4.8)×(18.9±2.0)	~2.5	706

^a The amounts of C16TABr, AgNO₃, AA and seed solution used for GNR growth are 0.54 g, 480 μL, 120 μL and 48 μL, respectively.

^b The concentration of additive in the growth solution used for GNR growth is 2.4 mM.

^c : the calculated concentration of GNRs (Orendorff and Murphy 2006)

^d: measured from Fig. 2a-e (At least 80 GNRs are counted for each set.)

318

319

320 **Table 3** Concentrations and LSPR peak wavelength of the GNR solutions prepared in the presence of aromatic
321 additive with addition of 300 μL (36 mmol) concentrated HCl ^a

Additive ^b (g)	C ^c (nM)	LSPR peak wavelength (nm)
PhOH	0.59	858
SA	0.61	890
5-BrSA	0.67	816
HNA	0.61	872
7-BrHNA	0.61	920

^a The amounts of C16TABr, AgNO₃, AA and seed solution used for GNR growth are 0.54 g, 480 μL , 300 μL and 48 μL , respectively.

^b The concentration of additive in the growth solution used for GNR growth is 2.4 mM.

^c: the calculated concentration of GNRs (Orendorff and Murphy 2006)

322

323

324 **Table 4** Experimental conditions used for controlled synthesis of GNRs and LSPR peak wavelengths of the GNR
325 solutions ^a

7-BrHNA (g, mM)	AgNO ₃ (mM)	HCl (mM)	AA (mM)	Seed solution (μL)	LSPR peak wavelength (nm)
0.08, 9.6	0.093	0	0.248	48	660
0.02, 2.4	0.031	0	0.248	48	714
0.08, 9.6	0.062	19.5	0.62	48	775
0.03, 3.6	0.062	19.5	0.31	48	835
0.04, 4.8	0.062	97.5	0.62	48	890
0.04, 4.8	0.093	97.5	0.62	96	960

^a The amounts of C16TABr used for GNR growth is 0.54 g.

326

327

328 **Figure caption**

329 **Fig. 1** Chemical structures of the five aromatic additives used in this study

330 **Fig. 2** Characterization of GNRs synthesized under the conditions specified in Table 1. TEM images of GNRs
331 synthesized using PhOH (a), SA (b) 5-BrSA (c), HNA (d), or 7-BrHNA (e) as additive. UV-vis-NIR spectra (f) of
332 GNRs synthesized using PhOH (I), SA (II), 5-BrSA (III), HNA (IV), or 7-BrHNA (V) as additive, respectively. The
333 photos (g) of GNR solutions synthesized using PhOH (I), SA (II), 5-BrSA (III), HNA (IV), or 7-BrHNA (V) as
334 additive, respectively. Scale bars: 100 nm

335 **Fig. 3** Characterization of GNRs synthesized under the conditions specified in Table 3. TEM images of GNRs
336 synthesized using PhOH (a), SA (b), 5-BrSA (c), HNA (d), or 7-BrHNA (e) as additive. UV-vis-NIR spectra (f) of
337 GNRs synthesized using PhOH (I), SA (II), 5-BrSA (III), HNA (IV), or 7-BrHNA (V) as additive, respectively. The
338 photos (g) of GNR solutions synthesized using PhOH (I), SA (II), 5-BrSA (III), HNA (IV), or 7-BrHNA (V) as
339 additive, respectively. Scale bars: 100 nm

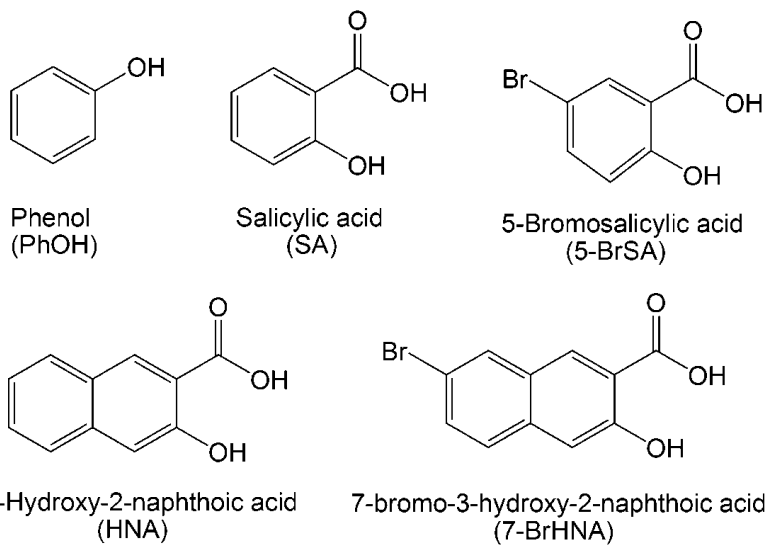
340 **Fig. 4** Fig. 4 Absorbances at 440 nm of the GNRs growth solutions v.s. time using different aromatic additives: PhOH
341 (a), SA (b), 5-BrSA (c), HNA (d), or 7-BrHNA (e) with the addition of HCl (lower pH) (solid circle) and without
342 addition of HCl (higher pH) (empty circle).

343 **Fig. 5** UV-vis-NIR spectra of GNRs synthesized by using PhOH (I), SA (II), 5-BrSA (III), HNA (IV), or 7-BrHNA (V)
344 as additive, in the presence of HNO₃.

345 **Fig. 6** Characterization of GNRs synthesized at different concentrations of 7-BrHNA as additive. UV-vis-NIR spectra
346 (a) and the LSPR peak wavelengths (b) of GNRs synthesized without addition of HCl, UV-vis-NIR spectra (c) and the
347 LSPR peak wavelengths (d) of GNRs synthesized with addition of 300 μ L HCl. The concentrations of 7-BrHNA in the
348 growth solution are 1.2 (I), 3.6 (II), 7.2 (III), 9.6 (IV) mM

349 **Fig. 7** Characterization of GNRs synthesized with 7-BrHNA as additive at different pH. UV-vis-NIR spectra (a) and
350 LSPR peak wavelengths (b) of the synthesized GNRs. The volumes of HCl added are 200 (I), 250 (II), 300 (III), 350
351 (IV) μ L

352 **Fig. 8** UV-vis-NIR spectra of the synthesized GNRs under the conditions in Table 4. The LSPR peaks of synthesized
353 GNRs are 660 nm (I), 714 nm (II), 775 nm (III), 835 nm (IV), 890 nm (V), or 960 nm (VI), respectively

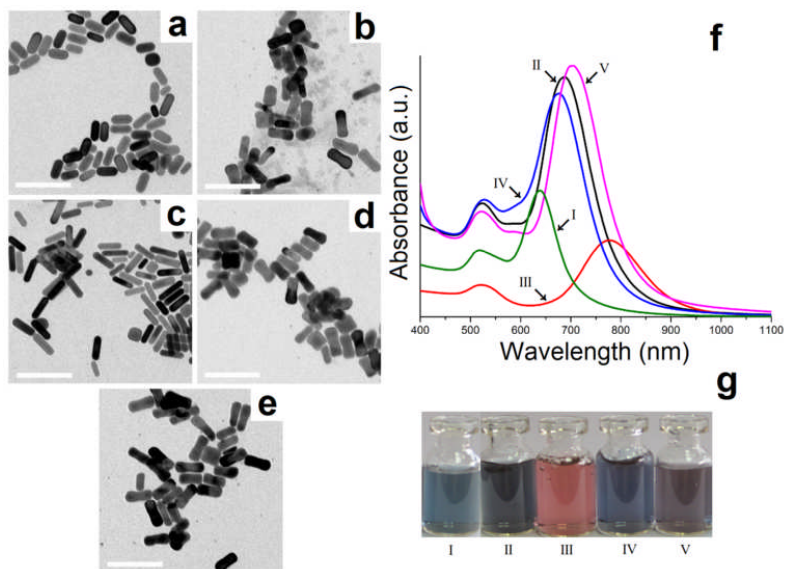


354

355 **Fig. 1** Chemical structures of the five aromatic additives used in this study

356

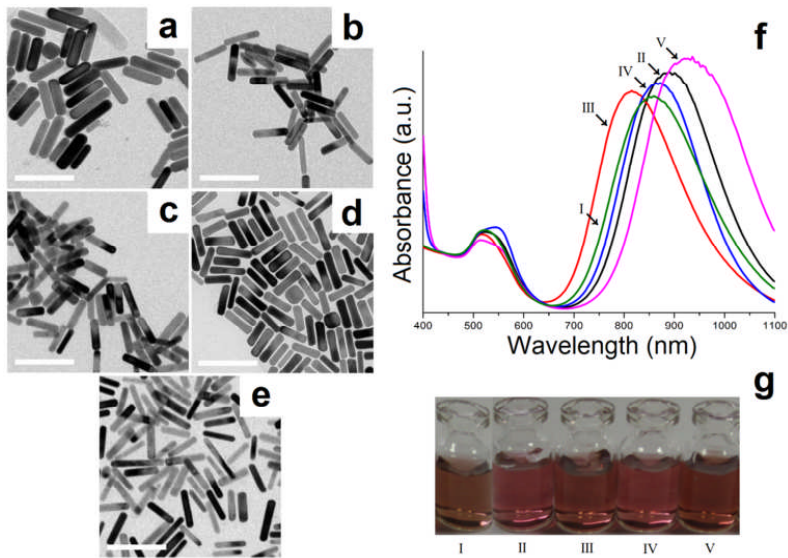
357



358

359 **Fig. 2** Characterization of GNRs synthesized under the conditions specified in Table 1. TEM images of GNRs
360 synthesized using PhOH (a), SA (b) 5-BrSA (c), HNA (d), or 7-BrHNA (e) as additive. UV-vis-NIR spectra (f) of
361 GNRs synthesized using PhOH (I), SA (II), 5-BrSA (III), HNA (IV), or 7-BrHNA (V) as additive, respectively. The
362 photos (g) of GNR solutions synthesized using PhOH (I), SA (II), 5-BrSA (III), HNA (IV), or 7-BrHNA (V) as
363 additive, respectively. Scale bars: 100 nm

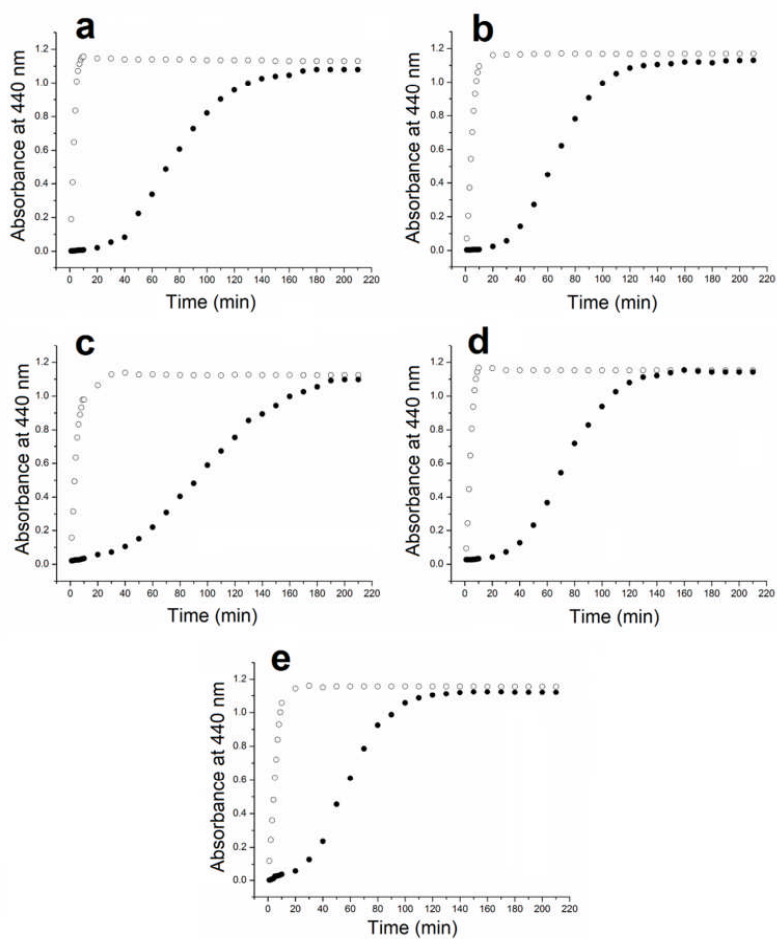
364



365
 366 **Fig. 3** Characterization of GNRs synthesized under the conditions specified in Table 3. TEM images of GNRs
 367 synthesized using PhOH (a), SA (b), 5-BrSA (c), HNA (d), or 7-BrHNA (e) as additive. UV-vis-NIR spectra (f) of
 368 GNRs synthesized using PhOH (I), SA (II), 5-BrSA (III), HNA (IV), or 7-BrHNA (V) as additive, respectively. The
 369 photos (g) of GNR solutions synthesized using PhOH (I), SA (II), 5-BrSA (III), HNA (IV), or 7-BrHNA (V) as
 370 additive, respectively. Scale bars: 100 nm

371
 372
 373
 374
 375
 376
 377
 378
 379
 380
 381

382



383

384 Fig. 4 Absorbances at 440 nm of the GNRs growth solutions v.s. time using different aromatic additives: PhOH (a),

385 SA (b), 5-BrSA (c), HNA (d), or 7-BrHNA (e) with the addition of HCl (lower pH) (solid circle) and without addition

386 of HCl (higher pH) (empty circle).

387

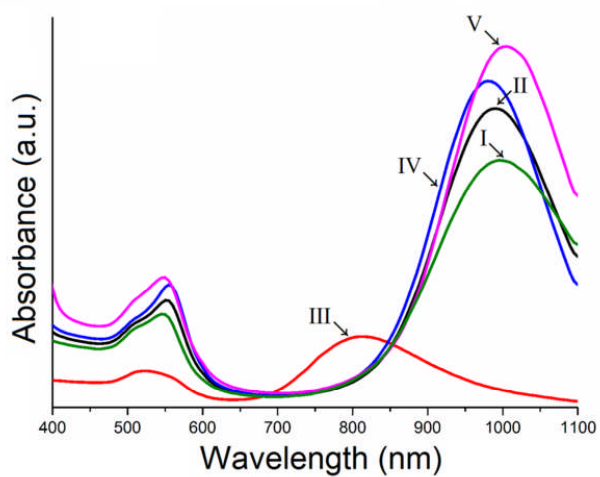
388

389

390

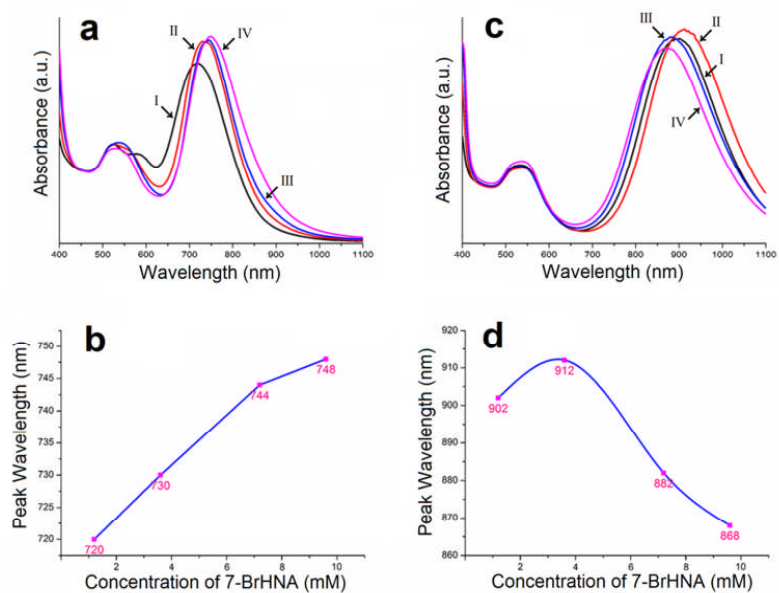
391

392
393
394
395



396
397
398
399
400

Fig. 5 UV-vis-NIR spectra of GNRs synthesized by using PhOH (I), SA (II), 5-BrSA (III), HNA (IV), or 7-BrHNA (V) as additive, in the presence of HNO_3 .



401

402 **Fig. 6** Characterization of GNRs synthesized at different concentrations of 7-BrHNA as additive. UV-vis-NIR spectra

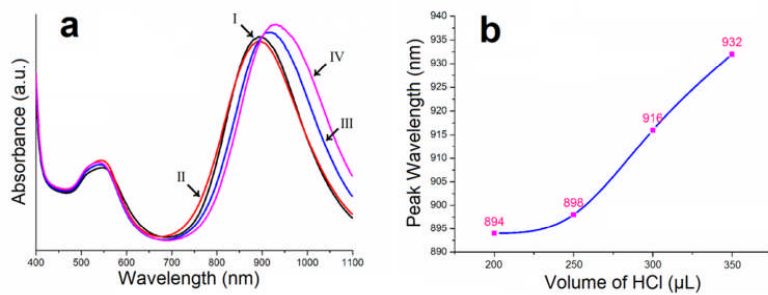
403 (a) and the LSPR peak wavelengths (b) of GNRs synthesized without addition of HCl, UV-vis-NIR spectra (c) and the

404 LSPR peak wavelengths (d) of GNRs synthesized with addition of 300 µL HCl. The concentrations of 7-BrHNA in the

405 growth solution are 1.2 (I), 3.6 (II), 7.2 (III), 9.6 (IV) mM

406

407

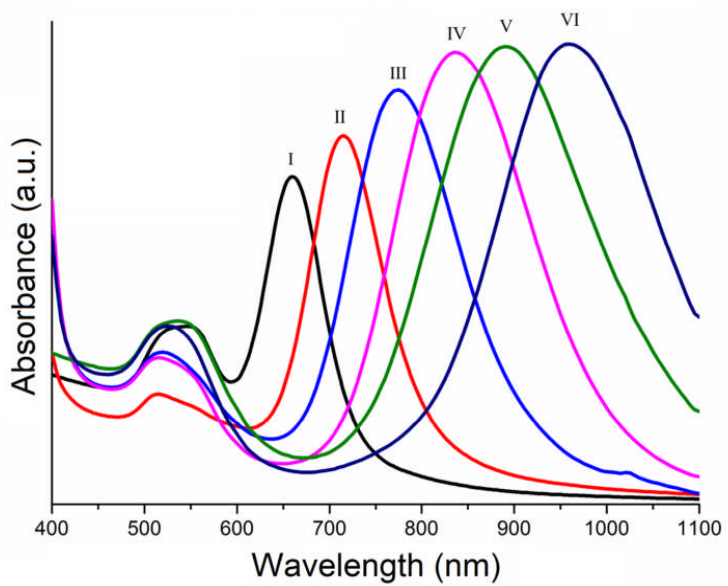


408

409 **Fig. 7** Characterization of GNRs synthesized with 7-BrHNA as additive at different pH. UV-vis-NIR spectra (a) and
410 LSPR peak wavelengths (b) of the synthesized GNRs. The volumes of HCl added are 200 (I), 250 (II), 300 (III), 350
411 (IV) μL

412

413



414

415 **Fig. 8** UV-vis-NIR spectra of the synthesized GNRs under the conditions in Table 4. The LSPR peaks of synthesized

416 GNRs are 660 nm (I), 714 nm (II), 775 nm (III), 835 nm (IV), 890 nm (V), or 960 nm (VI), respectively